



Article

Study of a gas disturbance mode content based on the measurement of atmospheric parameters at the heights of the mesosphere and lower thermosphere

Sergey Leble^{1*} , Sergey Vereshchagin^{1*} , Nataliya V. Bakhmetieva^{2*} and Gennadiy I. Grigoriev^{2*}

¹ Immanuel Kant Baltic Federal University, 236004, Nevskogo 14, Kaliningrad, Russia

² Lobachevsky State University of Nizhny Novgorod, Radiophysical Research Institute, Bolshaya Prechrskaya St., 25/12a, Nizhny Novgorod, 603950, Russia

* lebleu@mail.ru, sergey.ver@gmail.com, nv_bakhm@nirfi.unn.ru, grig19@list.ru

Abstract: The main result of this work is the estimation of the entropy mode accompanying a wave disturbance, observed at the atmosphere heights range of 90-120km. The study is the direct continuation and development of recent results on diagnosis of the acoustic wave with the separation on direction of propagation. The estimation of the entropy mode contribution relies upon the measurements of the three dynamic variables (the temperature, density and vertical velocity perturbations) of the neutral atmosphere measured by the method of the resonant scattering of radio waves on the artificial periodic irregularities of the ionospheric plasma. The measurement of the atmosphere dynamic parameters has been carried out on the SURA heating facility. The mathematical foundation of the mode separation algorithm is based on the dynamic projecting operator technique. The operators are constructed via the eigenvectors of the coordinate evolution operator of the transformed system of balance equations of the hydro-thermodynamics.

Keywords: exponential atmosphere; acoustic wave; diagnostics; projection operators; artificial periodic irregularities; neutral temperature; density

1. Introduction

The idea of a fluid perturbation decomposition goes up to the celebrated paper [1] related to a turbulent flow and studies of the nonlinear viscous and heat conducting compressible gas were formulated in [2], where the wave and non-wave components notions and a perturbation were formulated. Interaction of the components was also introduced.

A general description of a fluid perturbation in respect to equilibrium is naturally divided by projections to linear evolution operator subspaces to be identified as the perturbations modes. Its mathematical formulation is given in [3] for the classic (1,2,3 kinds) boundary conditions, see also recent book [4]. Its spectral content is determined by a kind of Fourier transform [5]. There are wave nonzero frequency ω and non-wave ($\omega = 0$) components [6]. The significance of the non-wave (entropy) component of a gas disturbance relates directly to the atmosphere warming phenomenon, for sudden stratosphere events [7] and for warming compendium look [8].

Appearance of the entropy mode is connected either with a heating phenomenon when energy transfer from waves of a large amplitude is implied [4] or when such mode is transported by wind or large scale (e.g. planetary) waves [9,10].

Such problem in plasma physics is more complicated due to the basic field components abundance with applications to the sun atmosphere physics [11,12]. A direct theory of the heating

phenomenon at plasma with mechanical and thermal losses and electrical resistivity is presented at [13]. The magnetoacoustic heating of plasma caused by periodic magnetosound perturbations with discontinuities is studied in a quasi-isentropic magnetic gas [14].

In algorithmic approach to mode definition [15,16] the method is formulated via projecting operators, that are defined for each evolution operator subspace. The projecting operators and their energy weight calculation are realised by means of an auxiliary norm introduction. The whole algorithm stages of a disturbance mode content diagnosis would outline below for the case of exponential atmosphere.

1. There are two possible classes of evolution operators that may be a base for the projecting procedure construction. One of them is evolution in time, say - t -evolution, for its applications [17]. The second is the z -evolution operator, both acting in the vector state. In our 1D case it is three-component one $\psi^T = (U, p, \rho)$ with the gas velocity (U), pressure (p) and density (ρ). The z -evolution equation reads

$$\psi_z = L\psi, \quad (1)$$

namely such form, that is derived in Sec. 3 defines the evolution operator L . The notations of the section differ because the dimensionless coordinates and entropy perturbation (instead of temperature) are introduced for further convenience.

2. Let consider now the eigen value task for the t -Fourier transform \tilde{L} of the evolution operator L having the matrix form

$$\tilde{L}\tilde{\psi} = k\tilde{\psi},$$

where $\psi \rightarrow \tilde{\psi}$ is the Fourier transform of the state vector.

3. For each eigenspace $\tilde{\psi}^i$, $i = 1, 2, 3$ it is convenient to introduce the matrix projecting operators P^i by means of the 3×3 eigen matrix $\Phi_{\alpha\beta} = \phi_\alpha^1 \phi_\beta^2$, $\alpha, \beta = 1, 2, 3$ so that the matrix elements [4]

$$P_{\alpha\gamma}^i = \Phi_{\alpha\beta} \Phi_{\beta\gamma}^{-1},$$

that are the functions of the frequency ω .

4. After the inverse Fourier transformation one can to apply the projecting technique to the observation data, otherwise, we transform the data by the discrete Fourier transformation, at the next step, we use the corresponding discretized projecting matrices $P_{\gamma\delta}^i$ to extract the data for the three modes (directed waves and entropy mode)

5. The energies of the directed and the entropy mode are estimated via discretized form of the general expression for energy of a gas perturbation. Its expression follow basic equations of the conservation law.

A role of the zero frequency mode is specific, because its propagation is determined by the simultaneous action of the nonlinearity and dissipation. Hence the mode (entropy mode) diagnostics by local measurements is a challenge as from theoretical point of view (asymmetry of derivatives entrance in basic equations) as from observations, due to its slow evolution [4].

While entropy mode account enters the main mechanism for some physical processes, such as non-linear heating, in other contexts it can be safely dropped out. And, because difficulty of its measurement and estimation, majority of models do just that. Generally, it is expected that it should be relatively insignificant in this case of the heights range under investigation. But we still want to obtain the value of it and to check those expectations. Proposed method could also be applied to other problems where its contribution is more pronounced. Even in the situation we examine, the mode growth with altitude may, potentially, lead to the essential change of the content of the atmosphere perturbation.

To solve this problem we rearrange equations of the basic system so as it to be a z -evolution one (Sec. 1 and [10]). This will allow us to find a projection operators for all three modes by the mentioned

algorithm. Also we will derive formula for an energy of the mode in the ω -space. Such results open the way to the local space diagnostics of acoustics and entropy modes.

For a source of observation data we take measurements of the velocity, temperature and the density of the neutral atmosphere in the height range 90-120 km by API (artificial periodic irregularities) technique. The technique is based on the resonant scattering of radio waves by induced periodic irregularities of the ionospheric plasma emerging in the field of a standing wave arising from the interference of the incident and reflected waves from the ionosphere [18,19]. The details of the physical base of the API is described in Sec. 2. The mathematical statement of the problem is given in the Sec. 3. Its reformulation as z-evolution problem is derived in Sec. 4. An expression for energy density is given at Sec. 6. The errors of measurements is given at Sec. 7 and the error of the whole estimation algorithm is described at the Sec. 8.

The main idea of this work is to prove, that the data on atmosphere parameters extracted from the SURA facility allow to estimate contributions of three mode (two waves and entropy). Other sources do not give such an opportunity.

Note, that in the paper [15] it was presented an alternative approach based on discrete projection operators. Also results in this paper were not applied to experimental data. The problem which was described there had only two wave modes without taking the entropy mode into account. The approach used to calculate energy in the article [15] was also more complex, we were able to find the means to greatly simplify this task.

Paper [16] also described two mode model, and do not contains ways to calculate an error estimation. This paper, while it is a logical continuation of the work done in [16] describes more precise three mode model, which allows to analyze entropy mode that is usually very hard task to do with real experimental data. It also includes an error estimations, both from experimental errors and ones from numerical method errors.

The book [17] describes basis of mathematics used in projection operators methods in several different fields of physics and do not contains specific projection operators or their application to the problem we study.

2. Experimental background

The estimation of the entropy mode contribution relies upon the measurements of three dynamic variables (the temperature, density and vertical velocity perturbations) of the neutral atmosphere obtained by the method of the resonant scattering of radio waves on the artificial periodic irregularities (APIs) of the ionospheric plasma [18–20]. The measurement of the atmosphere dynamic parameters has been carried out on the SURA heating facility (56.11°N; 46.1°E) which is situated near Nizhny Novgorod, Russian Federation. The facility creates artificial disturbances in the ionosphere influenced on a radio wave propagation. Powerful radio waves radiated into the ionosphere disturb the temperature and electron density. This causes many different “heating” effects in the ionospheric plasma, which are described in detail in reviews [21,22]. The creation of artificial periodic irregularities in the field of a powerful standing radio wave is among them. The API technique is described in detail in [18]. The scattering of probe radio waves by these irregularities has resonant properties, that is, the signal received from the API has significant amplitude when the frequencies and polarizations of the powerful and probe radio waves are same. After the end of the artificial impact on the ionosphere, APIs disappear during the relaxation time. A large level of scattered signal with a signal-to-noise ratio of the order of 10-100 allows one to determine atmospheric parameters with high accuracy. The altitude-time resolution is 1 km in altitude and 15 s in time and makes it possible to study short-term and long-term processes in the ionosphere and in neutral atmosphere.

The method for determining the temperature and density of the neutral atmosphere based on the analysis of the height dependence of the relaxation time of the API scattered signal is described in detail in [18,19]. At altitudes of 90–120 km, the API relaxation occurs under the influence of the

ambipolar diffusion [18,22]. The amplitude and phase of the scattered signal at the stage of relaxation of inhomogeneities are measured. The relaxation time is determined by the expression

$$\tau^* = \frac{1}{K^2 D} = \frac{M_i v_{im}}{K_B (T_{e0} + T_{i0}) K^2} = \frac{M_i v_{im}}{2 K_B T K^2} \quad (2)$$

where K_B is the Boltzmann constant, $K = 4\pi/\lambda$ is the wavenumber of the standing wave, $\lambda = \lambda_0/n$ is the wavelength in the propagation environment, n is the refractive index, D is the ambipolar diffusion coefficient, M_i is the molecular mass of the ion, T_{e0} and T_{i0} are the unperturbed electron and ion temperatures, and v_{im} is the frequency of collisions between ions and neutral molecules. It is considered that in the mid-latitude at mesosphere and the lower thermosphere heights $T_{e0} = T_{i0} = T$ up to the height 120–130 km, where T is the temperature of the neutral component. The expression for τ^* underlies the determination of many parameters of the lower ionosphere and the neutral atmosphere, including its temperature and density [18,19]. The atmospheric temperature and density are determined from the API relaxation time, which is inversely proportional to the ambipolar diffusion coefficient. Many results of studying the altitude–temporal variations of temperature and density in different geo- and helio-physical conditions are presented in [23–28]. To learn more about the API technique and in detail the methodology for determining the atmospheric temperature and density, we recommend reading [18,19]. The velocity of the vertical motion of the plasma is determined from the dependence of the phase on time. This velocity in the mesosphere and lower thermosphere is equal to the velocity of the neutral component, since the plasma at these altitudes is a passive admixture and moves with the neutrals.

The measured phase ϕ of the scattered signal can be written as $d\phi/dt = 2\pi F_d = 4\pi V/\lambda$ where F_d is the Doppler velocity and V is the velocity of the vertical movement of the neutral medium. Then the vertical velocity can be determined by the formula,

$$V = \frac{\lambda}{4\pi} \cdot \frac{d\phi}{dt} = \frac{c}{4\pi n f} \cdot \frac{d\phi}{dt} \quad (3)$$

where f is the frequency of the powerful and probing waves. Positive velocity values correspond to downward movement. To eliminate random errors associated with a change in the phase of the scattered signal due to the influence of natural noise on the scattered signal, the linear part of the approximation of the $\phi(t)$ dependence is used for the velocity calculation.

3. Mathematical statement of the problem formulation

Following [6] we start from the linearized conservation equations describing one-dimensional flow along the vertical axis z in terms of the deviations of pressure p' , density ρ' and velocity U' , from corresponding equilibrium stationary values \bar{p} , $\bar{\rho}$, \bar{U} . In the exponentially stratified atmosphere they take the form,

$$\bar{p}(z) = p_0 \exp(-z/H) = \rho_0 g H \exp(-z/H), \quad \bar{\rho}(z) = \rho_0 \exp(-z/H), \quad \bar{U} = 0,$$

where H is the height scale of stratification, p_0 and ρ_0 are the values of pressure and density at the zero z level, g - gravity acceleration. This system can be written in form

$$\frac{\partial U'}{\partial t} = -\frac{1}{\bar{\rho}} \frac{\partial p'}{\partial z} - \frac{\rho'}{\bar{\rho}} g \quad (4)$$

$$\frac{\partial p'}{\partial t} = -U' \frac{d\bar{p}}{dz} - \gamma \bar{p} \frac{\partial U'}{\partial z} \quad (5)$$

$$\frac{\partial \rho'}{\partial t} = -U' \frac{d\bar{\rho}}{dz} - \bar{\rho} \frac{\partial U'}{\partial z} \quad (6)$$

In one-dimensional exponentially stratified model presented in this paper the external force is described as the constant gravity acceleration g which is directed opposite to axis z , though it can be generalised to other mass forces including non-inertial ones. The flow of an ideal gas is considered, whose internal energy ϵ in terms of pressure and density takes the form

$$\epsilon = \frac{p}{(\gamma - 1)\rho}, \quad (7)$$

where $p = \bar{p} + p'$, $\rho = \bar{\rho} + \rho'$ i.e. full value is the sum of unperturbed value plus perturbation and $\gamma = C_p/C_v$ denotes specific heat ratio. The relation between the equilibrium pressure and density follows from the zero order stationary equality

$$\frac{d\bar{p}}{dz} = -g\bar{\rho}(z). \quad (8)$$

This linearized 1D equations for perturbations of pressure p' , density ρ' and gas velocity U' now can be simplified by introducing the new variable $\phi' = p' - \gamma \frac{\bar{p}}{\bar{\rho}} \rho'$ and then we can switch to this variables, conventionally used for the exponentially stratified atmosphere model:

$$\begin{aligned} P &= p' e^{z/2H}, \\ \Phi &= \phi' e^{z/2H}, \\ U &= U' e^{-z/2H}, \\ \varrho &= \rho' e^{z/2H}, \\ T_p &= T e^{-z/2H} \end{aligned} \quad (9)$$

where z is vertical coordinate and H is the height of the stationary atmosphere. That transforms the system (4-6) to the form

$$\frac{\partial U}{\partial t} = \frac{1}{\rho_0} \left(\frac{\gamma - 2}{2\gamma H} - \frac{\partial}{\partial z} \right) P + \frac{\Phi}{\gamma H \rho_0}, \quad (10)$$

$$\frac{\partial P}{\partial t} = -\gamma g H \rho_0 \left(\frac{\partial U}{\partial z} \right) - g \rho_0 \frac{\gamma - 2}{2} U, \quad (11)$$

$$\frac{\partial \Phi}{\partial t} = -(\gamma - 1) \rho_0 g U. \quad (12)$$

where ρ_0 denotes the density at the model lower boundary $z = 0$.

System (10-12) describes three-mode problem with two wave modes and one stationary entropy mode.

We can rewrite system (10-12) using the variable which are measured by API technique using relations

$$\Phi = P - \gamma \frac{p_0}{\rho_0} \varrho$$

since $\frac{p_0}{\rho_0} = \frac{\bar{p}}{\bar{\rho}}$ in exponentially stratified atmosphere and Mendeleev-Clapeyron's law (V^* is the gas volume)

$$p' = \frac{R}{\mu} (\bar{\rho} T + \rho' \bar{T}) \quad (13)$$

since $\bar{p} = \frac{R}{\mu} \bar{T} \bar{\rho}$ in Mendeleev-Clapeyron's law for nonperturbed atmosphere and after dropping out non-linear terms we get

$$P = \frac{R}{\mu} (\rho_0 T_p + \varrho \bar{T}) \quad (14)$$

It is convenient to rewrite system (10-12) in the terms of dimensionless functions and variables. To do this we shall use the uniform atmosphere height H and the velocity of sound $c = \sqrt{\gamma g H}$ as dimension parameters which gives time scale $H/c = \sqrt{\frac{H}{\gamma g}}$ so that the new dimensionless variables are

$z = H\xi, t = \tau \cdot H/c = \tau \sqrt{\frac{H}{\gamma g}}$. Functions are redefined as $U = cV = V\sqrt{\gamma g H}$, $P = p_0 \hat{p}$ and, since the Φ too has the pressure as dimension (because $\phi' = p' - \gamma \frac{\bar{p}}{\rho} \rho'$ and $\Phi = \phi' \cdot e^{z/2H}$) and $\Phi = p_0 \hat{\phi}$. After isolation of terms with $\frac{\partial}{\partial \tau}$ and taking into account that $p_0 = gH\rho_0$ we'll get

$$\frac{\partial V}{\partial \tau} = \frac{1}{\gamma^2} \left[\left(\frac{\gamma}{2} - 1 - \gamma \frac{\partial}{\partial \xi} \right) \hat{p} + \hat{\phi} \right], \quad (15)$$

$$\frac{\partial \hat{p}}{\partial \tau} = - \left(\frac{\gamma}{2} - 1 + \gamma \frac{\partial}{\partial \xi} \right) V, \quad (16)$$

$$\frac{\partial \hat{\phi}}{\partial \tau} = -(\gamma - 1) V. \quad (17)$$

4. Atmosphere gas disturbance initiation by a boundary regime

Let's transform our task into the boundary mode z-propagation form. It is easy to isolate spatial differentials for \hat{p} and V :

$$\frac{\partial}{\partial \xi} \hat{p} = \frac{\gamma - 2}{2\gamma} \hat{p} - \gamma \frac{\partial V}{\partial \tau} + \frac{1}{\gamma} \hat{\phi}, \quad (18)$$

and

$$\frac{\partial}{\partial \xi} V = -\frac{\gamma - 2}{2\gamma} V - \frac{1}{\gamma} \frac{\partial \hat{p}}{\partial \tau}, \quad (19)$$

but initial equation for $\frac{\partial \hat{\phi}}{\partial \tau}$, (17) does not contain $\frac{\partial}{\partial \xi} \hat{\phi}$. We can obtain it from the third equation in the form

$$\frac{\partial^2 \hat{\phi}}{\partial \tau \partial \xi} = -(\gamma - 1) \frac{\partial V}{\partial \xi}. \quad (20)$$

$$\frac{\partial \hat{\phi}}{\partial \xi} = \frac{(\gamma - 1)(\gamma - 2)}{2\gamma} \int V d\tau + \frac{\gamma - 1}{\gamma} \hat{p}. \quad (21)$$

Integral should not be a problem since it has rather simple form after Fourier transformation.

Finally, the system (18)-(19) and (21) takes the form

$$\frac{\partial}{\partial \xi} \begin{pmatrix} V \\ \hat{p} \\ \hat{\phi} \end{pmatrix} = L \begin{pmatrix} V \\ \hat{p} \\ \hat{\phi} \end{pmatrix} \quad (22)$$

where L is the z-propagation matrix operator, that gains the form

$$L = \begin{pmatrix} -\frac{\gamma-2}{2\gamma} & -\frac{1}{\gamma} \frac{\partial}{\partial \tau} & 0 \\ -\gamma \frac{\partial}{\partial \tau} & \frac{\gamma-2}{2\gamma} & \frac{1}{\gamma} \\ \frac{(\gamma-1)(\gamma-2)}{2\gamma} I_\tau & \frac{\gamma-1}{\gamma} \hat{p} & 0 \end{pmatrix} = \frac{1}{2\gamma} \begin{pmatrix} -(\gamma-2) & -2\frac{\partial}{\partial \tau} & 0 \\ -2\gamma^2 \frac{\partial}{\partial \tau} & (\gamma-2) & 2 \\ (\gamma-1)(\gamma-2) I_\tau & 2(\gamma-1) & 0 \end{pmatrix}, \quad (23)$$

where $I_\tau \kappa = \int \kappa d\tau$. To obtain the mode projection operators we need to transform (22) into Fourier space. At the domain the propagation matrix takes the form

$$\tilde{L} = \frac{1}{2\gamma} \begin{pmatrix} -(\gamma-2) & -2I\omega & 0 \\ -2\gamma^2 I\omega & (\gamma-2) & 2 \\ \frac{(\gamma-1)(\gamma-2)}{I\omega} & 2(\gamma-1) & 0 \end{pmatrix}. \quad (24)$$

5. Projection operators

Propagation matrix \tilde{L} (24) has the eigenvalues

$$0, \quad \frac{1}{2}\sqrt{1-4\omega^2}, \quad -\frac{1}{2}\sqrt{1-4\omega^2} \quad (25)$$

which are consistent with expected two directed waves, with up- and downward directions, and one stationary entropy mode. We can calculate projection operators using standard method $P_{ij}^k = E_{ik}E_{kj}^{-1}$ where E is a matrix constructed from eigenvectors. They take the form

$$P^1 = \frac{1}{\gamma^2(4\omega^2-1)} \begin{pmatrix} -4(\gamma-1) & 0 & -4I\omega \\ \frac{2I}{\omega}(\gamma-1)(\gamma-2) & 0 & 2(\gamma-2) \\ \frac{I}{\omega}(\gamma-1)(4\omega^2\gamma^2-(\gamma-2)^2) & 0 & 4\omega^2\gamma^2-(\gamma-2)^2 \end{pmatrix}, \quad (26)$$

$$P^2 = \frac{1}{4\gamma^2\omega^3K^3} \begin{pmatrix} \omega(1-K)Z_+ & -4I\omega^4\gamma K & 2I\omega^2(K^3-K) \\ -IX_+Z_+ & -\frac{X_+\omega^3\gamma K^2}{K-1} & 2X_+(K+K^2)\omega \\ I(\gamma-1)(K-1)Z_+ & 4(\gamma-1)\gamma\omega^3K^2 & -2(K^3-K)(\gamma-1)\omega \end{pmatrix}, \quad (27)$$

$$P^3 = \frac{1}{4\gamma^2\omega^3K^3} \begin{pmatrix} -\omega(1+K)Z_- & 4I\omega^4\gamma K & -2I\omega^2(K^3-K) \\ IX_-Z_- & \frac{X_-\omega^3\gamma K^2}{K+1} & -2X_-(K+K^2)\omega \\ -I(\gamma-1)(K-1)Z_- & -4(\gamma-1)\gamma\omega^3K^2 & 2(K^3-K)(\gamma-1)\omega \end{pmatrix}, \quad (28)$$

where $K = \sqrt{1-4\omega^2}$, $Z_{\pm} = (2\omega^2(\mp 4\gamma^2\omega^2 \pm \gamma^2 \mp 2\gamma \pm 4 + 2k\gamma) + (\gamma-2)(k+1))$, $X_{\pm} = \pm 2\gamma\omega^2 + k \pm 1$. Variables K , Z_{\pm} and X_{\pm} were introduced only to shorten notation of projection operators.

6. The mode energy density at omega-domain

Following [6] we get the formula for the energy density

$$\epsilon(z, t) = \rho_0 U(z, t)^2 + \frac{P(z, t)^2}{\gamma g H \rho_0} + \frac{\Phi(z, t)^2}{\gamma(\gamma-1)gH\rho_0}, \quad (29)$$

in the three-mode case. This formula is written using variables from (z, t) -space, so we need to rewrite it, using Fourier-images of these variables from (ω, τ) -space. Firstly, we must transform it into dimensionless form. To do it we will use the same formulas that we used for main system: $z = H\tilde{\zeta}$, $t = \tau \cdot H/c = \tau \sqrt{\frac{H}{\gamma g}}$, $P = p_0 \hat{p} = \rho_0 g H \hat{p}$, $U = cV = V \sqrt{\gamma g H}$ and $\Phi = p_0 \hat{\phi} = \rho_0 g H \hat{\phi}$. We get the expression

$$\epsilon(\tilde{\zeta}, \tau) = \rho_0 \gamma g H V (\tilde{\zeta}, \tau)^2 + \frac{(\rho_0 g H \hat{p}(\tilde{\zeta}, \tau))^2}{\gamma g H \rho_0} + \frac{(\rho_0 g H \hat{\phi}(\tilde{\zeta}, \tau))^2}{\gamma(\gamma-1)gH\rho_0}. \quad (30)$$

A transition to the ω -space variables by the conventional Fourier transformations

$$\hat{\phi}(\tilde{\zeta}, \tau) = \frac{1}{\sqrt{2\pi}} \int_{-\infty}^{\infty} e^{I\omega\tau} \tilde{\phi}(\tilde{\zeta}, \omega) d\omega, \quad (31)$$

$$\tilde{V}(\tilde{\zeta}, \tau) = \frac{1}{\sqrt{2\pi}} \int_{-\infty}^{\infty} e^{I\omega\tau} V(\tilde{\zeta}, \omega) d\omega, \quad (32)$$

and

$$q(\tilde{\zeta}, \tau) = \frac{1}{\sqrt{2\pi}} \int_{-\infty}^{\infty} e^{I\omega\tau} \tilde{q}(\tilde{\zeta}, \omega) d\omega. \quad (33)$$

We plug it in the expression for energy density (30) and get

$$\begin{aligned} \epsilon(\xi, \tau) = & \rho_0 g H \left[\gamma \frac{1}{\sqrt{2\pi}} \int_{-\infty}^{\infty} e^{I\omega\tau} \tilde{V}(\xi, \omega) d\omega \cdot \frac{1}{\sqrt{2\pi}} \int_{-\infty}^{\infty} e^{I\omega'\tau} \tilde{V}(\xi, \omega') d\omega' + \right. \\ & + \frac{1}{\gamma} \frac{1}{\sqrt{2\pi}} \int_{-\infty}^{\infty} e^{I\omega\tau} \tilde{p}(\xi, \omega) d\omega \cdot \frac{1}{\sqrt{2\pi}} \int_{-\infty}^{\infty} e^{I\omega'\tau} \tilde{p}(\xi, \omega') d\omega' + \\ & \left. + \frac{1}{\gamma(\gamma-1)} \frac{1}{\sqrt{2\pi}} \int_{-\infty}^{\infty} e^{I\omega\tau} \tilde{\phi}(\xi, \omega) d\omega \cdot \frac{1}{\sqrt{2\pi}} \int_{-\infty}^{\infty} e^{I\omega'\tau} \tilde{\phi}(\xi, \omega') d\omega' \right]. \end{aligned} \quad (34)$$

Hence, the energy ξ -profile is obtained by the integration over dimensionless time

$$E(\xi) = \int_{-\infty}^{\infty} \epsilon(\xi, \tau) d\tau. \quad (35)$$

It depends on ξ instead of τ since we are solving boundary mode ξ -propagation problem. But by definition

$$\int_{-\infty}^{\infty} e^{I\omega'\tau} e^{I\omega\tau} d\tau = 2\pi\delta(\omega + \omega'), \quad (36)$$

hence

$$E(\xi) = \int_{-\infty}^{\infty} \left[\gamma \tilde{V}^2(\xi, \omega) \omega^2 + \frac{1}{\gamma} \tilde{p}^2(\xi, \omega) + \frac{1}{\gamma(\gamma-1)} \tilde{\phi}^2(\xi, \omega) \right] d\omega. \quad (37)$$

7. Neutral atmosphere parameters obtained using API technique

As well as in work [16] we used the results of determining atmospheric temperature and density on 26 September 2017 from 12:00 to 16:20 local time (Moscow time) at the height at 100 km, adding to them the results of simultaneous measurements of the vertical velocity. Experimental data take the form of measurements of temperature, density and vertical gas velocity. Our projection operators are formulated in the terms of V , \hat{p} and $\hat{\phi}$. Vertical gas velocity can be used after calculating difference from average, transforming into dimensionless variables using formula $U = V\sqrt{\gamma g H}$. Then the discrete Fourier transformation was applied.

For the wave entropy variable $\tilde{\phi}$ we have $\hat{\phi} = \hat{p} - \frac{\gamma}{\rho_0} \rho$ where ρ is perturbations of density, it can be calculated as deviation from average too.

So, the only question is how to go over from temperature to \hat{p} which is perturbation of pressure. To do that we calculate pressure in each point using Mendelev-Clapeyron law

$$P = \frac{R}{\mu} \rho T$$

and then calculate difference with averaged value over all points to get perturbations values.

Experimental data are presented in the table

Time	Velocity; m/s	Temperature; K	Density; kg/m^3
12:00:00	-6.84E-01	2.19E+02	6.52E-07
12:05:00	-1.05E+00	1.82E+02	5.72E-07
12:10:00	-1.42E+00	1.45E+02	4.91E-07
12:15:00	-1.78E+00	1.08E+02	4.11E-07
12:20:00	-2.30E+00	2.14E+02	7.22E-07
12:25:00	-9.87E-01	1.29E+02	4.18E-07
12:30:00	-1.12E+00	1.50E+02	4.47E-07
12:35:00	-1.24E+00	1.71E+02	4.76E-07
12:40:00	-1.28E+00	1.29E+02	4.18E-07
12:45:00	-1.32E+00	1.36E+02	4.44E-07
12:50:00	3.80E-01	1.83E+02	4.70E-07
12:55:00	5.09E-01	2.09E+02	5.90E-07
13:00:00	6.37E-01	2.36E+02	7.09E-07

Time	Velocity; m/s	Temperature; K	Density; kg/m^3
13:05:00	-2.89E+00	1.69E+02	5.17E-07
13:10:00	-1.46E+00	2.32E+02	7.65E-07
13:15:00	-9.16E-01	1.39E+02	4.60E-07
13:20:00	-6.51E-01	1.54E+02	4.86E-07
13:25:00	-3.87E-01	1.68E+02	5.13E-07
13:30:00	-1.22E-01	1.83E+02	5.39E-07
13:35:00	1.43E-01	1.97E+02	5.65E-07
13:40:00	-3.56E+00	1.20E+02	3.74E-07
13:45:00	-7.34E-01	1.34E+02	3.80E-07
13:50:00	-6.30E-02	1.55E+02	3.28E-07
13:55:00	-9.07E-01	1.16E+02	3.01E-07
14:00:00	7.90E-02	6.92E+01	1.55E-07
14:05:00	3.85E-01	1.76E+02	5.04E-07
14:10:00	1.28E+00	9.90E+01	2.22E-07
14:15:00	1.15E+00	2.08E+02	5.12E-07
14:20:00	-1.39E+00	1.50E+02	3.71E-07
14:25:00	5.09E-01	2.12E+02	5.45E-07
14:30:00	-4.72E-01	1.60E+02	3.57E-07
14:35:00	-5.59E-01	2.16E+02	4.51E-07
14:40:00	5.23E-01	2.86E+02	6.36E-07
14:45:00	-8.27E-02	1.68E+02	6.28E-07
14:50:00	-2.19E+00	1.89E+02	5.11E-07
14:55:00	-8.93E-01	1.66E+02	6.72E-07
15:00:00	-7.24E-01	1.72E+02	5.88E-07
15:05:00	1.21E+00	1.98E+02	6.92E-07
15:10:00	-1.13E+00	1.49E+02	5.04E-07
15:15:00	-2.17E+00	1.82E+02	7.72E-07
15:20:00	-2.02E+00	2.14E+02	1.04E-06
15:25:00	-3.40E-01	8.96E+01	4.41E-07
15:30:00	4.87E+00	9.32E+01	4.46E-07
15:35:00	-1.09E+00	1.09E+02	4.53E-07
15:40:00	-1.71E+00	8.76E+01	2.78E-07
15:45:00	-2.33E+00	1.86E+02	6.93E-07
15:50:00	8.68E-01	1.30E+02	4.19E-07
15:55:00	-2.37E+00	1.96E+02	7.12E-07
16:00:00	-9.78E-01	2.01E+02	2.82E-07
16:05:00	1.97E-01	1.76E+02	4.59E-07
16:10:00	-2.35E+00	1.51E+02	6.36E-07
16:15:00	-2.04E+00	1.53E+02	4.50E-07
16:20:00	-1.73E+00	1.55E+02	2.64E-07

Now it is possible to apply out projection operators (26,27,28) and then to calculate separately energies for each mode using formula (37) which need to be rewritten in the discrete form by replacement of integrals with sums i.e. using midpoint rule. Since points are spaced and we are interested in relative values only, simple sums can be used. It gives us relative values. For entropy mode we obtain

$$E_1 \approx 0.000024E \quad (38)$$

and for the wave modes we have

$$E_2 \approx 0.501E, \quad (39)$$

$$E_3 \approx 0.499E, \quad (40)$$

where $E = E_1 + E_2 + E_3$ is the total energy of all modes.

In contrast to the work [16], we used the data of determination of three atmospheric quantities; we use a set that allows us to find the contribution of the entropy mode. An important fact is that it turned out to be small. In addition, we have demonstrated the procedure for measuring this contribution. Recall that the origin of the entropy mode is heating by waves, and which is proportional to the dissipation and the square of the amplitude of this mode. At these altitudes, both are few.

8. Error estimation

8.1. The vertical velocity measurement error

Our analysis has been carried out with a certain degree of accuracy. The error in the E estimates is the sum of the errors in measuring the parameters of the neutral component (temperature, density, and vertical velocity) by the API technique and the error in the algorithm for calculating the entropy and wave modes.

As can be seen from the formula for the vertical velocity, the absolute error ΔV of a single measurement of the speed is determined by the error of the time derivative of the signal phase. If we find $\Delta\phi/\Delta t$ from two dimensions, then the variance of this derivative is expressed by the formula

$$\sigma_{\Delta\phi/\Delta t}^2 = \frac{1}{t_1}(\sigma_{\phi_1}^2 + \sigma_{\phi_2}^2) \quad (41)$$

where the time measurement error is neglected, and $\sigma_{\phi_1}^2$ and $\sigma_{\phi_2}^2$ are the variances of the first and second measurements, t_1 is the measurement time.

To reduce the error, it is necessary to increase the measurement time interval t_1 , but this is prevented by the exponential decrease in the signal amplitude during the API relaxation period, which leads to a decrease in the signal-to-noise ratio (A/A_{noise}) and an increase in the variance $\sigma_{\phi_2}^2$. According to [29], for $A/A_{\text{noise}} > 3$ the value of σ_{ϕ}^2 is $\sigma_{\phi_2}^2 \approx (A/A_{\text{noise}})^2$ therefore $\sigma_{\Delta\phi/\Delta t}^2 = \sigma_{\phi_1}^2 \frac{1+\exp(t_1/\tau^*)}{t_1}$. This value reaches a minimum at $t_1 = 0.86\tau^*$ and gives the value $\sigma_{\Delta\phi/\Delta t}^2 = 3\sigma_{\phi_1}^2$.

A more accurate estimate of the derivative can be obtained by taking into account all measured values of the phase ϕ . It was shown in [20] that the optimal procedure for finding $\Delta\phi/\Delta t$ is a linear approximation of $\phi(t)$ by the least squares method with the weight function $\exp(-t_1/\tau^*)$ while

$$\sigma_{\Delta\phi/\Delta t}^2 \rightarrow \frac{2\sigma_{\phi}}{\tau^*} \sqrt{\frac{2\Delta t}{\tau^*}} \quad (42)$$

at $t_1 \gg \tau^*$. Ultimately, the error in determining the vertical speed is expressed by the formula

$$\Delta V = \frac{\lambda}{4\pi} \frac{A_{\text{noise}}}{A} \frac{1}{\tau^*} \sqrt{\frac{2\Delta t}{\tau^*}} \quad (43)$$

Assuming the relaxation time of the scattered signal equal to $\tau^* = 1$ s the time between two measurements $\Delta t = 20$ ms and $A/A_{\text{noise}} = 20$, which corresponds to the API experiments, we find the value $\Delta V = 0.08 = 0.08$ m/s. Thus, the random error of a single measurement does not exceed 0.1 m/s. There is a small systematic error due to the heating of the electron gas by a powerful radio wave. This issue is considered in detail in [18]. It was shown there that for typical experimental conditions at an altitude of 100 km, the systematic error in measuring the velocity does not exceed $\Delta V = 0.05$ m/s for the extraordinary component of a powerful wave. The total relative velocity error does not exceed 2%.

8.2. Errors in determining neutral temperature and density

In [18,19] a method for determining the temperature and density of the neutral component based on measurements of the height-time dependencies of the amplitude of the signal scattered by the API technique is considered in detail. Let us to explain briefly how the errors in determining the atmospheric parameters were calculated. Based on the expression of the barometric dependence of pressure on altitude in an isothermal $\rho(H) = \rho_0 \exp[-(h - h_0)/H]$, $H = K_B T / mg$, where H is the height of a homogeneous atmosphere, K_B is the Boltzmann constant, and measuring the relaxation time τ^* at two close (to satisfy the isothermal condition) heights h_1 and h_2 , taking into account the dependence of the wave vector k on the height h through the refractive index n of a powerful wave in plasma $k = k_0 n(h)$, we obtain for H the expression

$$H = \frac{h_2 - h_1}{\ln(n^2 \tau_1^*(h_1)) - \ln(n^2 \tau_2^*(h_2))} \quad (44)$$

The values of the relaxation time τ^* are determined by the decay of the amplitude of the scattered signal by a factor of e with a step in height of 1 km.

The neutral temperature T is determined from the relation $T = mgh/K_B$, respectively, the absolute error in determining the temperature is $\Delta T = mg\Delta h/K_B$ and the relative error is $\delta T = \delta H$. To find the value of H , a linear approximation of the function $\ln(n^2 \tau^*) = b_0 h + b_1$ over several values of the relaxation time is used. Coefficients b_0 and b_1 are determined by the least squares method by applying the linear regression method to the dependence $\ln(n^2 \tau^*)$. In this case, the standard (root-mean-square) approximation error is calculated in the usual way [30]. For most measurements by the API method, the relative error $\delta T = \delta H$ does not exceed 5%. The error in determining the density ρ is of the same order of magnitude and does not exceed 10% [19,20]. As the long-term measurements of atmospheric parameters by the API method show, only in some cases can these errors reach 20%.

8.3. Algorithm error

Algorithm, described in this paper inevitably also introduce additional error. It is impossible to definitely restore function by the limited set of points without making some propositions about function, which are not always possible to do. We will try to evaluate which error are introduced by this process of restoration. This error appears even for pure waves.

To estimate it we used a method based on Runge's approach - we recalculated all our energies using only subset of our data points. The resulting relative error was the estimated as

$$\delta_1 E = \left| \frac{E_N - E_{N/2}}{E_N} \right| \quad (45)$$

There E_N denotes value of energy calculated using N data points. $E_{N/2}$ - using only odd numbered points. Error do not noticeable change if we use complimentary subset of points (i.e. even numbered points) which confirm correctness of such method of error estimation.

Resulting error was around 49% for entropy mode and around 0.9% for wave modes. Therefore

$$E_1 \approx (0.000024 \pm 49\%)E, \quad (46)$$

and for wave modes

$$E_2 \approx (0.501 \pm 0.9\%)E, \quad (47)$$

$$E_3 \approx (0.499 \pm 0.9\%)E. \quad (48)$$

We have used the results of the energy density estimation at the heights within the nearest vicinity of the experimental conditions (about $z = 100\text{km}$). The estimation is performed in the frequency domain,

that we consider as upper boundary of the error because of the minimum contribution of white noise while the Fourier transformation is performed.

9. Conclusion

The main purpose of this work is the estimation of the entropy mode accompanying a wave disturbance, observed at the atmosphere heights range of 90-120km. The study is the direct continuation and development of recent results on diagnosis of the acoustic wave with the separation on direction of propagation. The estimation of the entropy mode contribution relies upon the measurements of the three dynamic variables (the temperature, density and vertical velocity perturbations) of the neutral atmosphere measured by the method of the resonant scattering of radio waves on the artificial periodic irregularities of the ionospheric plasma. The measurement of the atmosphere dynamic parameters have been carried out on the SURA heating facility. The mathematical foundation of the mode separation algorithm is based on the dynamic projecting operator technique. The operators are constructed via the eigenvectors of the evolution operator of the transformed system of balance equations of the hydro-thermodynamics.

The main result is the algorithmic extraction of the modes of an atmosphere gas disturbance, specifically: the entropy mode from three-component data of atmospheric parameters. Having in mind the vertical movements of the atmosphere gas within rather small height interval, we apply the 1D exponential model of the atmosphere that results in relatively simple algorithm of the mode contribution extraction. The entropy mode energy estimation, as it is calculated at the Sec. 7 give values, small, compared to ones of wave modes. We consider it as important result, expecting however the mode contribution growth, that may be an important reason for the background temperature and density slow dynamics, which, as mentioned, should be taken into account in thermosphere heating or cooling during strong atmosphere storms. A reason for such growth may be a presence of wave perturbation of high enough amplitude. It is important as for atmosphere perturbations modeling as for prognosis.

10. Funding

Funding: N.V.B. and G.I.G. were supported by the Russian Science Foundation under grant 20-17-00050

11. Conflicts of Interest

Conflicts of Interest: The authors declare no conflict of interest. The funders had no role in the design of the study; in the collection, analyses, or interpretation of data; in the writing of the manuscript; or in the decision to publish the results

12. Author Contributions

Author Contributions: Conceptualization, S.L.; methodology, S.L., S.V. and N.V.B.; software, S.V.; validation, S.L., N.V.B. and G.I.G.; formal analysis, S.L. and S.V.; investigation, S.L., N.V.B., G.I.G. and S.V.; resources, N.V.B.; data curation, N.V.B.; writing—original draft preparation, S.L. and S.V.; writing—review and editing, S.L., project administration, S.L. All authors have read and agreed to the published version of the manuscript.

1. Kovasznay, Leslie S. G. "Turbulence in Supersonic Flow". *Journal of the Aeronautical Sciences*. 20 (10), pp. 657–674., 1953 <https://doi.org/10.2514/8.2793>
2. Chu, Boa-Teh; Kovásznay, Leslie S. G. "Non-linear interactions in a viscous heat-conducting compressible gas". *Journal of Fluid Mechanics*. 3 (5) p. 494., 1958, <https://doi.org/10.1017/S0022112058000148>.

3. Brezhnev, Yu.; Kshevetsky, S.; S.V. Leble. Linear initialization of hydrodynamical fields, *Atmospheric and Oceanic Physics* **1994**, 30(10), 84–88. https://www.researchgate.net/publication/262766717_Linear_Initialization_of_hydrodynamical_fields
4. S. Leble, A. Perelomova, S. Leble, A. Perelomova, Dynamical projectors method in hydro- and electrodynamics. CRC Press, Taylor and Frensis group, 564p, 2018, <https://doi.org/10.1201/9781351107990>.
5. Leble, S.; Vereshchagin, S. A Wave Diagnostics in Geophysics: Algorithmic Extraction of Atmosphere Disturbance Modes , *Pure and Applied Geophysics*, Volume 175, Issue 8, pp.3023-3035, 2018, <https://doi.org/10.1007/s00024-018-1808-y>
6. S. Leble, A. Perelomova “Problem of proper decomposition and initialization of acoustic and entropy modes in a gas affected by mass force ”, *Applied Mathematical modelling* 37 pp. 629-635, 2013, <https://doi.org/10.1016/j.apm.2012.02.037>
7. Sun, L.; Robinson, W. A.; Chen, G. The predictability of stratospheric warming events: more from the troposphere or the stratosphere?; *Journal of the Atmospheric Sciences* **2012**, 69(2), 768–783. <https://doi.org/10.1175/JAS-D-11-0144.1>
8. Butler, A. H.; Sjoberg, J. P.; Seidel, D. J.; Rosenlof, K. H. A sudden stratospheric warming compendium, *Earth System Science Data* **2017**, 9 (1), 63–76. <https://doi.org/10.5194/essd-9-63-2017>.
9. Pedloski, J. *Geophysical fluid dynamics*; Springer-Verlag, New York, 1987. <https://doi.org/10.1007/978-1-4612-4650-3>
10. Gordin, A.V. *Mathematical problems of hydrodynamical weather prediction. Analytical aspects*; Gydrometeoizdat [in Russian], Leningrad, 1987.
11. K. Murawski et al. Entropy mode at a magnetic null point as a possible tool for indirect observation of nanoflares in the solar corona . *Astronomy and Astrophysics*, 2011, <https://doi.org/10.1051/0004-6361/201116942>
12. Liang Qian et al. Entropy modes in multi-component plasmas confined by a dipole field. *Physics of Plasmas*, 2020. <https://doi.org/10.1063/1.5119519>
13. Anna Perelomova, On description of periodic magnetosonic perturbations in a quasi-isentropic plasma with mechanical and thermal losses and electrical resistivity, *Physics of Plasmas* 27, 032110 (2020); <https://doi.org/10.1063/1.5142608>
14. Anna Perelomova, Magnetoacoustic heating of plasma caused by periodic magnetosound perturbations with discontinuities in a quasi-isentropic magnetic gas, *Archives of Acoustics* 45(2), 241-251 (2020) <https://doi.org/10.24425/aoa.2020.133145>
15. S. B. Leble, S. D. Vereshchagin, and I. S. Vereshchagina. Algorithm for the Diagnostics of Waves and Entropy Mode in the Exponentially Stratified Atmosphere. *Russian Journal of Physical Chemistry B*, 2020, Vol. 14, No. 2, pp. 371–376. © Pleiades Publishing, Ltd., 2020. Russian Text © The Author(s), 2020, published in *Khimicheskaya Fizika*, 2020, Vol. 39, No. 4, pp. 73–79. <https://doi.org/10.1134/S199079312002027X>
16. Sergey Leble, Sergey Vereshchagin, Nataliya V. Bakhmetieva and Gennadiy I. Grigoriev. On the Diagnosis of Unidirectional Acoustic Waves as Applied to the Measurement of Atmospheric Parameters by the API Method in the SURA Experiment. *Atmosphere* 2020, 11, 924; <https://doi.org/10.3390/atmos11090924>
17. Leble, S.B. *Nonlinear waves in waveguides with stratification*; Springer-Verlag, Berlin, 1990. <https://doi.org/10.1007/978-3-642-75420-3>
18. Belikov, V.V.; Benediktov, E.A.; Tolmacheva, A.V.; Bakhmet'eva, N.V. Ionospheric Research by Means of Artificial Periodic Irregularities; Copernicus GmbH: Katlenburg-Lindau, Germany, 2002; p. 160.
19. Benediktov, E. A., V. V. Belikov, Yu. N. Grebnev, and A. V. Tolmacheva (1993), Determination of the temperature and density at heights of the ionospheric E-layer, *Geomagn. Aeron. (in Russian)*, 1993, V. 33. No 5, 170-174.
20. Belikov, V.V. Approximation of experimental data of the exponent // *Izvesiya Vyzov. Radiofizika*. 1993. V.36, No12, 1105-1112. – (In Russian)
21. Belikov V.V., Grach S.M., Karashtin A.N., Kotik D.S., Tokarev Yu.V The "Sura" facility: Study of the atmosphere and space (a review). *Radiophys. Quantum Electron*. 2007, 50, p. 497–526; <https://doi.org/10.1007/s11141-007-0046-4>
22. Frolov V.L., Bakhmet'eva N.V., Belikov V.V., Vertogradov G.G., Vertogradov V.G., Komrakov G.P., Kotik D.S., Mityakov N.A., Polyakov S.V., Rapoport V.O., Sergeev E.N., Tereshchenko E.D., Tolmacheva A.V., Uryadov V.P,

- Khudukon B.Z. Modification of the earth's ionosphere by high-power high-frequency radio waves. *Phys. Usp.* 2007, 50, p. 315–324; <https://doi.org/10.1070/PU2007v050n03ABEH006282>
23. N. V. Bakhmetieva, V. D. Vyakhirev, G. I. Grigoriev, M. N. Egerev, E. E. Kalinina, A. V. Tolmacheva, I. N. Zhemyakov, G. R. Vinogradov, and K. M. Yusupov. Dynamics of the Mesosphere and Lower Thermosphere Based on Results of Observations on the SURA Facility // *Geomagnetism and Aeronomy*, 2020, Vol. 60, No. 1, pp. 96–111. © Pleiades Publishing, Ltd., 2020. Russian Text © The Author(s), 2020, published in *Geomagnetizm i Aeronomiya*, 2020, Vol. 60, No. 1, pp. 99–115. <https://doi.org/10.1134/S001679322001003X>
 24. Bakhmet'eva N.V., Bubukina V.N., Vyakhirev V.D., Kalinina E.E., Komrakov G.P. Response of the lower ionosphere to the partial solar eclipses of August 1, 2008 and March 20, 2015 based on observations of radio-wave scattering by the ionospheric plasma irregularities // *Radiophysics and Quantum Electronics*. 2017. V. 59. No 10. pp. 782-793. <https://doi.org/10.1007/s11141-017-9747-5>
 25. Nataliya V. Bakhmetieva, Gennady I. Grigoriev, Ariadna V. Tolmacheva, and Ilia N. Zhemyakov. Investigations of Atmospheric Waves in the Earth Lower Ionosphere by Means of the Method of the Creation of the Artificial Periodic Irregularities of the Ionospheric Plasma // *Atmosphere*, 2019, V.10, No 8, p.450; <https://doi.org/10.3390/atmos10080450>
 26. Grigor'ev, G.I.; Bakhmetieva, N.V.; Tolmacheva, A.V.; Kalinina, E.E. Relaxation time of artificial periodic irregularities of the ionospheric plasma and diffusion in the inhomogeneous atmosphere. // *Radiophys. Quantum Electron.* 2013, 56, 187–196. <https://doi.org/10.1007/s11141-013-9425-1>
 27. Bakhmetieva, N.V.; Grigor'ev, G.I.; Tolmacheva, A.V.; Kalinina, E.E. Atmospheric turbulence and internal gravity waves examined by the method of artificial periodic irregularities. *Russ. J. Phys. Chem. B* 2018, 12, p. 510–521. <https://doi.org/10.7868/S0207401X18050023>
 28. Bakhmetieva N.V., Bubukina V.N., Vyakhirev V.D., Grigoriev G.I., Kalinina E.E., Tolmacheva A.V. The Results of Comparison of Vertical Motion Velocity and Neutral Atmosphere Temperature at the Lower Thermosphere Heights // *Russ. J. Phys. Chem.* 2017. V. 11. No 6. pp. 1017–1023. <https://doi.org/10.7868/S0207401X17120056>
 29. Tikhonov, V.I. Statistical radio technique (in Russian); Soviet Radio: Moscow, 1966, p.687.
 30. Julius S. Bendat, Allan G. Piersol. Random Data: Analysis and Measurement Procedures, 4th Edition. – Wiley Series in Probability and Statistics. March 2010. 640 Pages. <https://www.wiley.com/en-am/9780470248775>. ISBN: 978-0-470-24877-5. <https://doi.org/10.1002/9781118032428>

© 2021 by the authors. Submitted to *Atmosphere* for possible open access publication under the terms and conditions of the Creative Commons Attribution (CC BY) license (<http://creativecommons.org/licenses/by/4.0/>).